12WCEE 2000

SOIL FRICTION RESTRAINT OF OBLIQUE PIPELINES IN LOOSE SAND

Tung-Wen HSU[1], Yuh-Jyh CHEN[2] And Chun-Yin WU[3]

SUMMARY

This paper presents the soil friction restraint on the oblique pipelines in loose sand. A series of experimental tests are conducted in a prefabricated large scale drag box with dimensions 1.83 m × 1.83 m × 1.22 m. Model pipes 0.61 m long with diameters of 152.4, 228.6, and 304.8 mm are obliquely moved from an axial-longitudinal to lateral-transversal direction in the drag box to study the associated soil restraints of the oblique pipes with various shallow embedded depths. All the test results indicate that for the axial pipes, the longitudinal soil restraint could be estimated as the product of the average of the vertical and horizontal earth pressures at the centerline of the pipe and the tangent value of soil-pipe friction angle, whereas for the lateral pipes, the transversal soil restraint could be predicted by using the limit equilibrium model with the assumption of the planar sliding failure surface. For the oblique pipes, the longitudinal soil restraint decreases, whereas the transversal soil restraint increases with the oblique angle, respectively. Besides, both soil restraints increase with the embedded depth. The longitudinal and transversal soil restraints of the oblique pipes could geometrically be obtained by multiplying the corresponding cosine and sine values of the oblique angle with the associated longitudinal soil restraint of axial pipe and the transversal soil restraint of lateral pipe, respectively. The findings also indicate that the scale effects are not significant for the size of the pipes tested herein.

INTRODUCTION

An evaluation of soil restraint or loading on pipelines in response to the differential ground movement in the adverse environment has been drawn attention by many pipeline designers. For design purposes, Nyman [6] catalogued four principal directions of buried pipeline restraints, which include vertical-uplift, horizontal-lateral, vertical-bearing, and longitudinal-axial. Among these, the axial soil friction restraint is considered as a critical parameter in the seismic design of straight buried pipelines. O'Rourke et al. [8] reported that the most probable failure modes for modern welded steel pipelines in the seismic damage are apparently due to the surface wave propagation and the permanent ground deformation (PGD). In order to evaluate seismic wave propagation effects on buried pipelines, O'Rourke and Hmadi [7] utilized the axial friction forces near the soil-pipeline interface to estimate the axial strain induced in the pipelines. In their analysis, it appears that the coefficient of friction at the soil-pipeline interface plays a significant factor on the determination of the maximum axial restraint on the pipelines. Similarly, O'Rourke et al. [8] also found that the response of buried pipelines due to the longitudinal PGD is connected with the wrinkling failure in the 1985 Mexico City Earthquake. Strain induced in the pipelines subjected to the longitudinal PGD is through the friction-like forces at the soil-pipe interface. The maximum axial force at the soil-pipe interface depends on the compaction condition of the surrounding soil and the coefficient of friction between sand and pipeline. In determining the magnitude of the coefficient of friction, the experimental results performed by Brumund and Leonards [3] were used. The test set-up consisted of a 127 mm (5 in.) diameter cylinder of sand encased in a rubber membrane with a 28.58 mm ($1^1/_8$ in.) diameter, 355.6 mm (14 in.) long rod installed along its axes. The normal stress was applied to the sand/rod interface by evacuating air from within the membrane. And the pressure at the sand/rod interface was equal to the vacuum induced membrane pressure. However, Kennedy [5] found that the normal pressure at the sand/rod interface in a large sample was about 1.4 times the pressure on the membrane. Besides, the in-placed pipelines are not always installed in such a way that its orientation is parallel to the direction of the longitudinal PGD.

[1] *Department of Civil Engineering, National Chung-Hsing University, Taichung 40227, TAIWAN.Email: twhsu@dragon.nchu.edu.tw*
[2] *Department of Civil Engineering, National Chung-Hsing University, Taichung 40227, TAIWAN*
[3] *Department of Civil Engineering, National Chung-Hsing University, Taichung 40227, TAIWAN*

Hence, it becomes pertinent to explicitly conduct the laboratory tests to measure the longitudinal soil restraint on the oblique pipelines.

The literature survey indicates that the published information regarding the longitudinal soil friction restraint on the oblique pipelines is not attainable. Most of the previous research was emphasized on the soil-pile friction resistance. The ASCE Committee on Gas and Liquid Fuel Lifelines [1] suggests the use of a elasto-plastic or a hyperbolic model for the soil resistance versus pipe movement. The analysis work done by O'Rourke and Hmadi [7] estimates that the maximum forces per unit length at the soil-pipeline interface f_m is equal to the multiplication of the coefficient of friction μ between the surrounding sand and pipeline as well as the product of the circumference and the average of the vertical and horizontal pressure on the pipe, which could be expressed as follows:

$$f_m = \mu\gamma z(\frac{1+\kappa_0}{2})\pi D \quad (1)$$

whereγ= unit weight of the soil; z = distance measured from the pipeline centerline to the ground surface; k_0 = coefficient of lateral earth pressure; and D = diameter of the pipeline. The coefficient of friction μ varies between 0.5tanψ and 1.0tanψ depending on the pipeline surface condition, where ψ is the internal friction angle of the soil. In examining the above equation, it was found that the coefficient of friction for various pipe surface conditions was described by the different magnitude of tanψ. The soil–pipe friction angle, which is frequently adopted by the geotechnical engineers, is not presented.

This study concentrates on the soil friction restraint of loose sand against the oblique longitudinal-transversal direction of the pipes. The inclination angles, α, ranging from 0° for pure axial to 90° for pure lateral motion as defined in Fig. 1, were varied in angular increments of 10° for each pipe recess depth test. Three sizes of pipe with diameters of 152.4 mm (6 in.), 228.6 mm (9 in.) and 304.8 mm (12 in.) were used. The shallow burial depths H/D ranged from 1 to 3 were tested, in which H is the recess depth of the pipe measured from the sand surface to the centerline of the pipe and D is the diameter of the pipe. Local sand from the Da-Du riverbed in the central area of Taiwan was used for all tests. Loose sand with density of 15.20 kN/m^3 (1.55 g/cm^3), corresponding with the direct shear internal friction angle of 33° (relative density of 21%), was prepared in this investigation. The exterior surface roughness of the pipes was that of a normal exposed pipe. The soil-pipe friction angle was determined by conducting the direct shear test with the pipe surface material placed in between the two shear boxes, in which the test sand were filled. The results indicate that the typical soil-pipe friction angle was about 21°, which is approximately 2/3 of the soil friction angle.

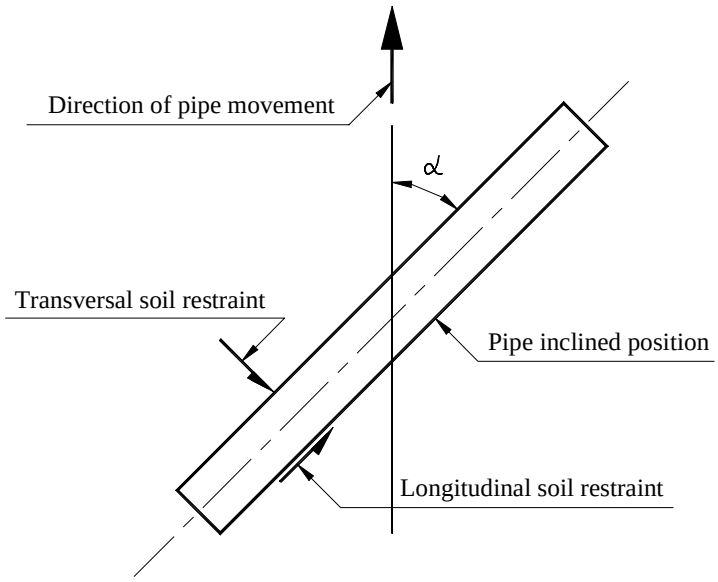

Fig. 1. Sketch of pipe oblique angle α.

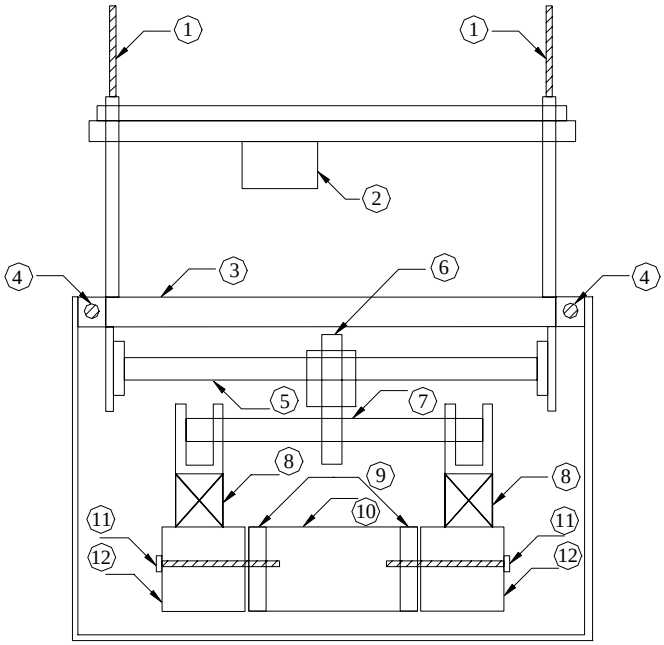

(a) Front view

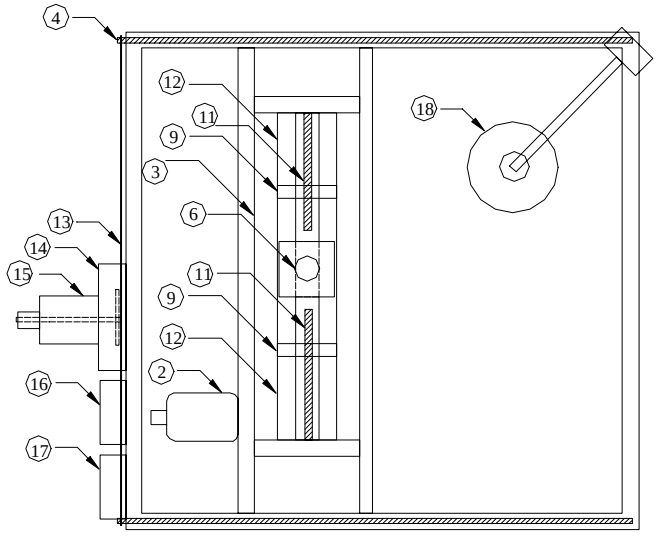

(b) Plan view

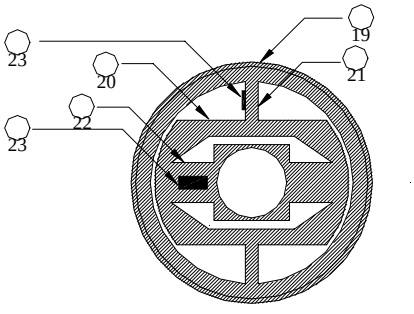

(c) Force transducer

1 Lead screw for vertical movement
2 Vertical drive motor
3 Platform
4 Lead screw for horizontal movement
5 Top frame
6 Pivot
7 Bottom frame
8 Bracing member
9 Force transducer
10 Instrumented Pipe
11 Long screw bolt
12 Adjoining pipe
13 Horizontal drive chain
14 Horizontal drive gear box
15 Horizontal drive motor
16 Horizontal speed controller box
17 Vertical speed controller box
18 Sand spreading hopper
19 Outer frame
20 Inner frame
21 Vertical strain gage bridge
22 Horizontal strain gage bridge

Fig. 2. (a)(b) Cross section of large scale drag box and (c) force transducer measurement system.

EXPERIMENTAL PROGRAM

All the pipe loading tests were conducted in a fabricated large-scale drag box with internal dimensions 1.83 m × 1.83 m × 1.22 m (6 ft × 6 ft × 4 ft). The movement of the pipe was controlled by the rotation of the lead screw actuated by the horizontal drive motor. The components of the test apparatus are described in detail in a companion paper (Hsu [4]). While measuring the axial soil friction restraint other than lateral soil restraint of the pipe, the way of the installation of the pipe in the test apparatus needs some modification. First, the pipe support system was newly developed and basically connected with two frames, the bottom frame supported the pipe, while the top frame was rigidly attached to the lower end of each vertical plate with a pivot joining these two frames. The vertical plate could be actuated by the vertical drive motor, thereby raising or lowering the pipe to the desired recess depth. For oblique pipe tests, the pivot could be rotated with respected to the top fixed frame so that the bottom frame which holds the pipe could be oriented to the desired inclination angle, α. Previous pipe loading tests[4] indicate that the least length to diameter ratio was 8:1 and the data would have resulted in significant end effects. To eliminate these effects, the strain gage transducers were redesigned. Besides, the arrangement of the transducers are such that the longitudinal soil restraint as well as the transversal soil restraint against the oblique motion pipe could also be measured simultaneously. To do this, a pair of newly force transducers were developed as shown in Fig. 2(c). These two transducers were installed inside the both ends of an active or instrumented 0.61-m (2-ft) long center section pipe, while the other two outer sections of 0.30-m (1-ft) adjoining pipes connected with the transducers through the long screw bolts. To ensure that the outer pipes align horizontally and also to deter any twisting during loading, these two outer pipes connected the bottom frame with vertical and diagonal bracing members to strengthen the longitudinal stiffness as shown in Figs. 2(a) and 2(b). Moreover, to prevent friction between the active and the adjoining pipes, a slight gap was left which was sealed around the pipe with silicone rubber compound. The strain gage arrangement on the transducers was fabricated such that the longitudinal and transversal forces were measured independently without interfering each other. As shown in Fig. 2(c), the two vertical strain gage bridges connected with the outer circular frame of the transducer measure the transversal soil restraint, while the other two horizontal strain gage bridges connected to the inner frame measure the longitudinal soil restraint. Here, the strain gages were attached on the side of the vertical bridges and the top of the horizontal bridges, respectively. Each test was performed at a constant rate of 2 cm/min. Owing to the limited depth of the drag box, three sizes of model pipes were used. (a) A 152.4-mm (6 in.) pipe was tested at recess depths of 1, 2, and 3; (b) a 228.6-mm (9-in.) pipe was tested at recess depths of 1 and 2; and (c) a 304.8-mm (12-in.) pipe was tested only at recess depth of 1. For investigating the size effects of the pipe on the soil restraint, the experimental results of associated longitudinal and transversal soil restraints for different size of oblique pipes at same recess depth will be grouped together and compared each other, respectively.

TEST RESULTS

Ultimate Resistance:

Force-displacement curves for the oblique motion pipe are typically shown in Figs. 3(a-b). For each oblique pipe loading test, the associated transversal soil force F_H and longitudinal soil force F_V are imposed on the pipe as

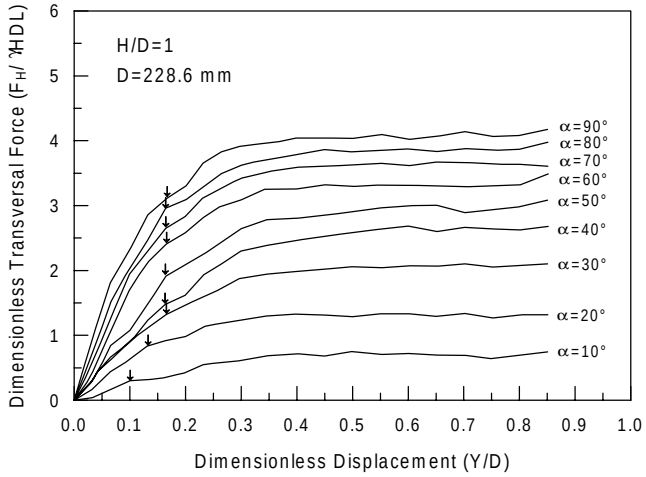

Fig. 3(a). Dimensionless transversal force $F_H/\gamma HDL$ versus dimensionless displacement Y/D for 228.6 mm pipe with H/D = 1.

shown in Fig. 1, respectively. In Figs. 3(a-b), the results have been plotted as the dimensionless force $F_H/(\gamma HDL)$ or $F_V/(\gamma HDL)$ versus dimensionless displacement Y/D, in which L = the pipe length; Y = the pipe displacement;

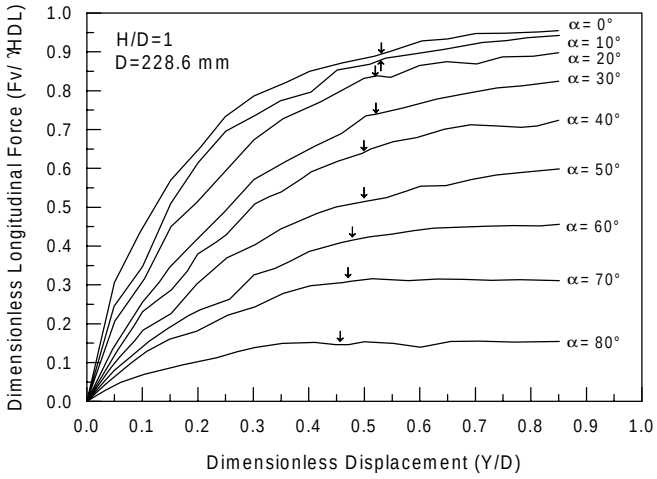

Fig. 3(b). Dimelsionless longitudinal force Fv/ γHDL versus dimensionless displacement Y/D for 228.6 mm pipe with H/D = 1.

and the other variables are the same as previously defined. As shown in the figures, the dimensionless ultimate force was defined at the point where the force-displacement curve has the maximum curvature. Arrows on the curves show the points representing the dimensionless ultimate transversal force F'_{HM} denoted as $F'_{HM} = F_{HM}/(\gamma HDL)$ or the dimensionless ultimate longitudinal force F'_{VM} denoted as $F'_{VM} = F_{VM}/(\gamma HDL)$, in which F_{HM} and F_{VM} are the ultimate transversal and longitudinal forces, respectively. It could be observed that F'_{HM} and F'_{VM} might not occur at the same pipe displacement. The results also indicate that F'_{HM} decreased, whereas F'_{VM} increased with the oblique angle as shown in Figs. 5(a) and 5(b), respectively.

Theoretical Analysis:

Transversal soil restraint of lateral pipeline (α=90°):

For estimating the transversal soil restraint of lateral pipeline (α=90°), an analogy is made between the resistance of the anchor plate and the restraint of pipeline subjected to the horizontal motion in sand. With the analogy of the projected anchor plate placed at the center line of the pipe, the implicit limit equilibrium model with the assumption of planar rupture surface was applied to predict the lateral soil restraint of the shallow buried pipes in loose sand (Hsu [4]). For the lateral pipe subjected to horizontal motion, the limit equilibrium model together with the force polygon in the soil wedge are shown in Figs. 4(a) and 4(b), respectively. The forces in the soil wedge are as follows: R_1 is the resultant of the lateral earth pressure at active stress state acting on the left side of the soil wedge; W is the weight of soil included in the entire soil wedge; and R_2 is the resultant of the shear and normal forces acting on the passive surface of sliding. For determining the transversal soil restraint of the lateral pipeline (α=90°), the trial sliding surface with different angles θ is varied until the minimum value of P_u is reached as shown in Fig. 4(b). The value of P_u could also be solved by the system of linear equations in the matrix form as follows:

$$\begin{bmatrix} 1 & -\cos(\theta-\phi) \\ 0 & \sin(\theta-\phi) \end{bmatrix} \begin{bmatrix} p_u \\ R_2 \end{bmatrix} = \begin{bmatrix} -R_1\cos\phi \\ W + R_1\sin\phi \end{bmatrix} \tag{2}$$

Longitudinal soil restraint of axial pipeline (α=0°):

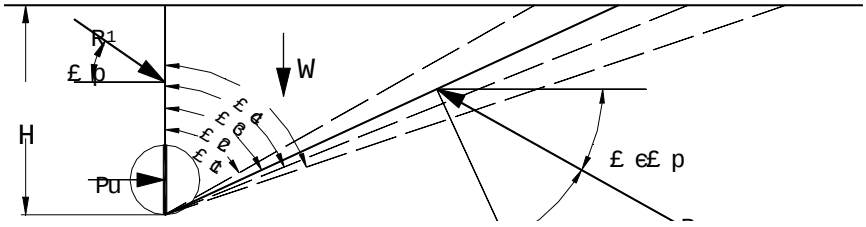

Fig. 4(a). Limits equilibrium model.

For determining the longitudinal soil restraint of axial pipeline (α=0°), it is necessary to estimate the coefficient of friction μ between sand and pipeline according to eq. (1). In doing this, the soil-pipe friction angle δ was obtained with an angle of 21° by simple shear test as described previously. The value of μ was alternatively expressed as tanδ in a geotechnical way. And the k_0 value was the coefficient of lateral earth pressure at rest, since no separation occurs between the pipe and the surrounding sand as the pipe moves. The longitudinal soil restraint of axial pipeline at various depths could then be determined following eq. (1).

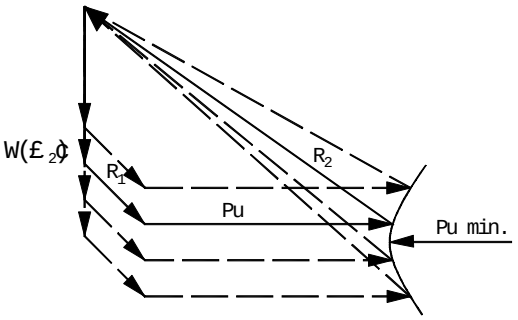

Fig. 4(b). Equilibrium of force polygon.

Scale Effects of Pipe Diameter:

For each recess depth, the test results were expressed as dimensionless ultimate transversal force F_{HM}' and dimensionless ultimate longitudinal force F_{VM}' versus oblique angle α, respectively. For comparison purposes, all test results of different size pipes at the same recess depth were grouped together to check the scale effects as shown in Figs. 5(a-b) and Figs. 6(a-b), respectively. It was found that the scale effects were minor for pipe diameters up to 304.8 mm (12 in.). These findings are consistent with the experimental results done by Audibert and Nyman [2], in which the scale effects were minor for the size of the pipe diameter up to 0.61 m (2 ft) in the lateral motion. It could also be noted that for any oblique angle test, both values of F'_{HM} and F'_{VM} increased with recess depth.

Comparison with Theoretical Predictions:

Previous theoretical analysis was focused on the associated soil restraints of two extreme cases of pipe orientation, which were lateral pipe (α=90°) and axial pipe (α=0°). For the lateral pipe, there is only transversal soil restraint imposed on the pipe and no any connection with the longitudinal soil restraint. The theoretical

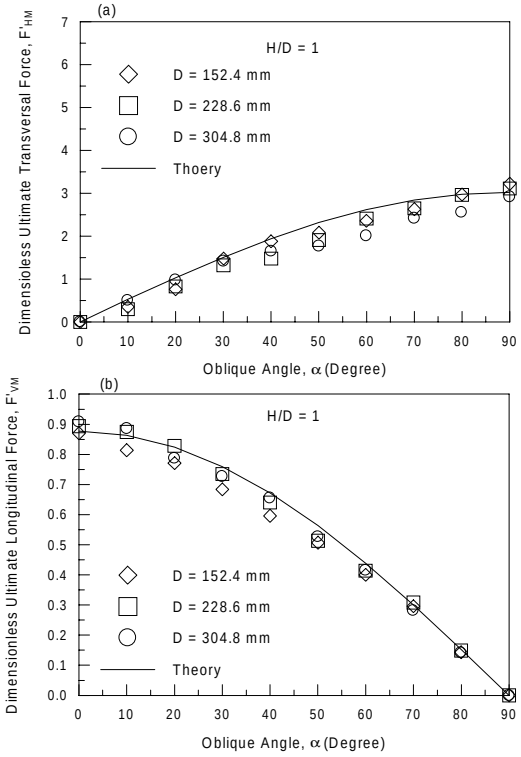

Fig. 5(a) Dimensionless ultimate transversal force F'_{HM} and (b) dimensionless ultimate longitudinal force F'_{VM} versus oblique angle α for different size pipes with H/D=1.

predictions indicate that the transversal soil restraint of lateral pipe could be determined by using the limit equilibrium model with the assumption of planar rupture surface. To extend its analysis to the inclined pipe, it is obvious that the transversal soil restraint of oblique angle pipe could be obtained by geometrically multiplying the corresponding sine value of the oblique angle with the associated transversal soil restraint of the lateral pipe. Figs. 5a-7a show the comparisons between the theoretical predictions and the experimental results for the relationship of the dimensionless ultimate transversal force versus the oblique angle where excellent agreement

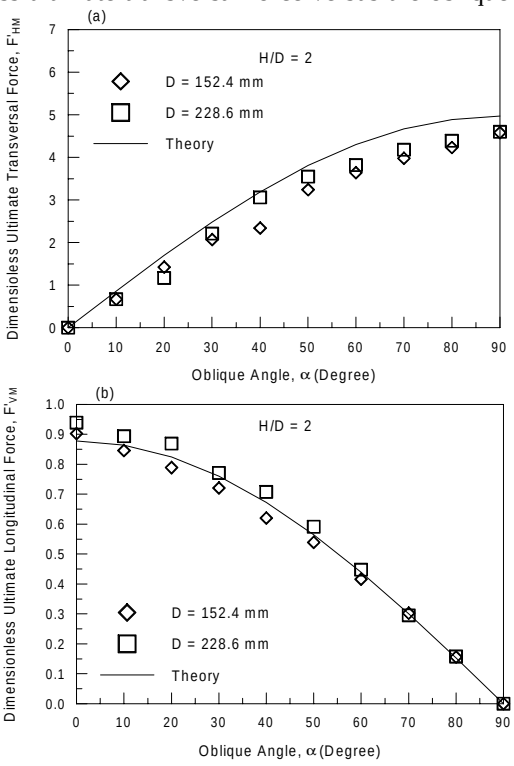

Fig. 6(a) Dimensionless ultimate transversal force F'_{HM} and (b) dimensionless ultimate longitudinal force F'_{VM} versus oblique angle α for different size pipes with H/D=2.

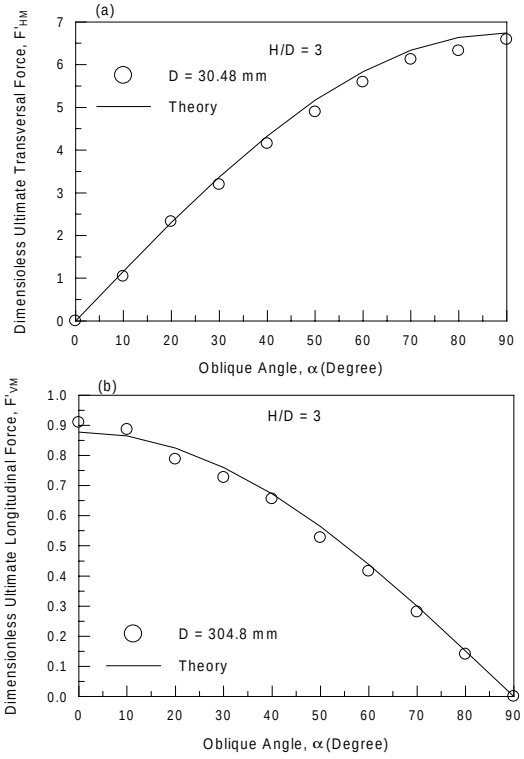

Fig. 7(a) Dimensionless ultimate transversal force F'_{HM} and (b) dimensionless ultimate longitudinal force F'_{VM} versus oblique angle α for 304.8 mm pipe with H/D=3.

can be noted. Similarly, for the axial pipe, there is only longitudinal soil restraint imposed on the pipe and no any connection with the transversal soil restraint. The theoretical estimation of the longitudinal soil restraint of the axial pipe was based on eq. (1), in which the coefficient of friction μ was expressed as $\tan\delta$ and the k_0 value was the coefficient of lateral earth pressure at rest. The longitudinal soil restraint of the oblique angle pipe appears to be equal to the multiplication of the corresponding cosine value of the oblique angle and the associated longitudinal soil restraint of the axial pipe. For comparison purposes, the longitudinal soil restraint of the oblique pipe was converted into the dimensionless term of F_{VM}'. The experimental findings and the theoretical predictions are in good agreement as shown in Figs. 5b-7b.

CONCLUSIONS

1. The transversal soil restraint of the lateral pipe was determined by using the limit equilibrium model with the assumption of the planar rupture surface.
2. The longitudinal soil restraint of the axial pipe was estimated as the product of the average of the vertical and horizontal earth pressures and the tangent value of soil-pipe friction angle at the centerline of the pipe.
3. The transversal soil restraint of the oblique pipes could geometrically be obtained by multiplying the corresponding sine value of the oblique angle with the associated transversal soil restraint of the lateral pipe.
4. The longitudinal soil restraint of the oblique pipes could geometrically be obtained by multiplying the corresponding cosine values of the oblique angle with the associated longitudinal soil restraint of the axial pipe.
5. The scale effects were minor for the size of the pipe diameter up to 304.8 mm.

ACKNOWLEDGEMENTS

This research was sponsored by the National Science Council of Taiwan under grant number NSC87-2218-E005-016. The writers wish to thank the financial support.

REFERENCES

1. ASCE Committee on Gas and Liquid Fuel Lifelines (1984), *Guidelines for the Seismic Design of Oil and Gas Pipeline Systems.*

2. Audibert, J.M.E. and Nyman, K.J. (1977), "Soil restraint against horizontal motion of pipes", *Journal of the Geotechnical Engineering Division, ASCE,* Vol. 103, No. GT10, pp1119-1142.

3. Brumund, W. and Leonards, G. (1973), "Experimental study of static and dynamic friction between sand and typical construction materials", *Journal of Testing and Evaluation,* Vol. 1, No. 2, pp162-165.

4. Hsu, T. W. (1996), "Soil restraint against oblique motion pipelines in sand", *Canadian Geotechnical Journal,* Vol. 33, No. 1, pp180-188.

5. Kennedy, D.J.L. (1961), "A study of the failure of liners for oil wells associated with compaction of producing strata", *Ph. D. Thesis, Graduate College, University of Illinois,* Urbana, Illinois.

6. Nyman, K.J. (1984), "Soil response against oblique motion of pipes", *Journal of Transportation Engineering,, ASCE,* Vol. 110, No. 2, pp190-202.

7. O'Rourke, M.J., El Hmadi, K. (1988), "Analysis of continuous buried pipelines for seismic wave effects", *Earthquake Engineering and Structural Dynamics,* Vol. 16, No. 6, pp917-929.

8. O'Rourke, M.J., Liu, X. and Flores-Berrones, R. (1995), "Steel pipe wrinkling due to longitudinal permanent ground deformation", *Journal of Transportation Engineering, ASCE,* Vol. 121, No. 5, pp443-451.